AIP | Applied Physics Letters

Active surfaces: Ferrofluid-impregnated surfaces for active manipulation of droplets

Karim S. Khalil, Seyed Reza Mahmoudi, Numan Abu-dheir, and Kripa K. Varanasi

Citation: Applied Physics Letters **105**, 041604 (2014); doi: 10.1063/1.4891439
View online: http://dx.doi.org/10.1063/1.4891439
View Table of Contents: http://scitation.aip.org/content/aip/journal/apl/105/4?ver=pdfcov
Published by the AIP Publishing

Active surfaces: Ferrofluid-impregnated surfaces for active manipulation of droplets

Karim S. Khalil,[1] Seyed Reza Mahmoudi,[1] Numan Abu-dheir,[2] and Kripa K. Varanasi[1,a)]
[1]*Department of Mechanical Engineering, Massachusetts Institute of Technology, Cambridge, Massachusetts 02139, USA*
[2]*Department of Mechanical Engineering, King Fahd University of Petroleum and Minerals, Dhahran 31261, Kingdom of Saudi Arabia*

(Received 29 May 2014; accepted 15 July 2014; published online 1 August 2014)

Droplet manipulation and mobility on non-wetting surfaces is of practical importance for diverse applications ranging from micro-fluidic devices, anti-icing, dropwise condensation, and biomedical devices. The use of active external fields has been explored via electric, acoustic, and vibrational, yet moving highly conductive and viscous fluids remains a challenge. Magnetic fields have been used for droplet manipulation; however, usually, the fluid is functionalized to be magnetic, and requires enormous fields of superconducting magnets when transitioning to diamagnetic materials such as water. Here we present a class of active surfaces by stably impregnating active fluids such as ferrofluids into a textured surface. Droplets on such ferrofluid-impregnated surfaces have extremely low hysteresis and high mobility such that they can be propelled by applying relatively low magnetic fields. Our surface is able to manipulate a variety of materials including diamagnetic, conductive and highly viscous fluids, and additionally solid particles. © *2014 AIP Publishing LLC*. [http://dx.doi.org/10.1063/1.4891439]

Droplet mobility and manipulation on non-wetting surfaces has received widespread attention due to its significance in a variety of applications such as liquid repellency,[1–6] anti-icing,[5,7–12] dropwise condensation,[13–17] and biomedical devices.[18–20] In most applications, droplets are normally moved passively, for example, using gravity.[2] Active manipulation of droplets using electric fields[21–24] and vibrational fields[25,26] have been studied, yet moving highly-conductive and viscous fluids remains difficult.[27–29] The use of magnetic fields for droplet and particle manipulation has been recently studied; however, the droplets are paramagnetic[30] or functionalized to be magnetic,[31,32] and the process becomes challenging for diamagnetic fluids as they need enormous magnetic fields using superconducting magnets to operate.[33–35] Here, we present a lubricant-impregnated surface,[36] where a textured solid is impregnated with a ferrofluid, that is able to manipulate a variety of different liquids including diamagnetic, viscous, electrically conductive and even solid particles. As illustrated in Figure 1(a), we create a liquid-solid composite surface that utilizes a spatially non-uniform magnetic field to drive the droplets. Since the magnetic property of the liquid does not impose any limitations on the proposed technique, we are able to transport diamagnetic liquids (here water) with the relatively small magnetic fields of permanent magnets.

Lubricant-impregnated surfaces have recently been shown to display low contact angle hysteresis,[36–42] self-cleaning,[38,43] dropwise condensation,[44–46] as well as anti-icing[47–49] and anti-fouling[50–54] properties, yet the lubricant that is being used has usually never been active. Here, a textured surface consisting of a micropost array with a coating of octadecyltrichlorosilane (OTS) is impregnated with a ferrofluid (EMG901, Ferrotec, Inc.). Ferrofluids, a colloidal suspension of ferromagnetic nanoparticles (~10 nm) in a carrier fluid stabilized by surfactant, have been studied extensively, but only rarely in their ability to manipulate free droplets.[55–57] The surface treatment of the ferromagnetic particles prevents agglomeration due to magnetic forces and short range van der Waals forces, and Brownian motion prevents particle sedimentation in both gravitational and magnetic fields. The surfactant surface treatment on the particles is stable generally up to a few years. In the absence of an applied field, the particles are randomly oriented giving the fluid no net magnetization. However, in the presence of an external magnetic field, ferromagnetic nanoparticles align their magnetic dipole moment parallel to the direction of the applied field and display a strong magnetic interaction.[55] The impregnated ferrofluid provides active manipulation for free droplets placed on the surface in several ways. The thermodynamically-stable states of a droplet on a lubricant-impregnated surface have been shown to depend on both the relative spreading coefficients of the lubricant and droplet, as well as the texture geometry.[36] A microtextured surface lends itself to a critical contact angle below which the lubricant will successfully impregnate the texture and remain held by capillary forces. The lubricant (here an oil-based ferrofluid, EMG901) will impregnate a textured surface if $\theta_{os(v)} \leq \theta_c$, where $\theta_{os(v)}$ is the contact angle of ferrofluid-lubricant "o" on the smooth solid "s" in the presence of air-vapor "v" and θ_c is the critical contact angle for impregnation, given by[36,37]

$$\theta_c = \cos^{-1}[(1-\phi)/(r-\phi)]. \quad (1)$$

Here, ϕ is the fraction of the projected area of the textured surface that is occupied by a solid and r is the ratio of total

a)Author to whom correspondence should be addressed. Electronic Mail: varanasi@mit.edu

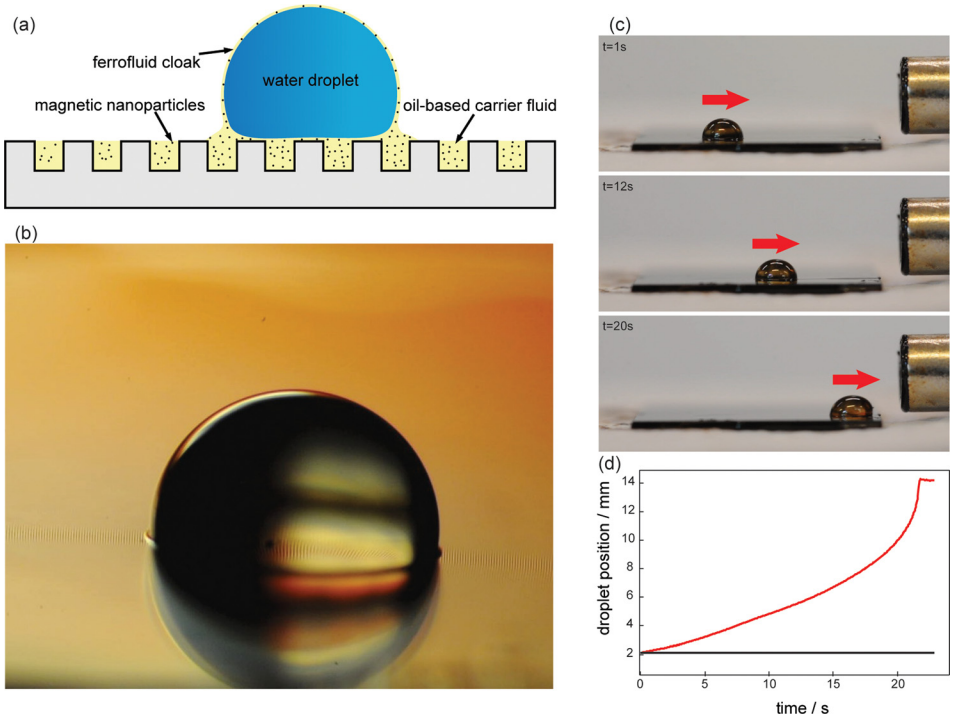

FIG. 1. Ferrofluid-impregnated textured surface. (a) Schematic of surface with water droplet resting on top. The ferrofluid can cloak the water droplet if the spreading coefficient ($S_{ow(v)} \geq 0$) is greater than 0. (b) Photograph of water droplet resting on the surface with the ferrofluid cloak. (c) Snapshots of droplet mobility experiment as water droplet is accelerated towards the magnet.[59] (d) Water droplet position versus time in mobility experiment (Multimedia view). [URL: http://dx.doi.org/10.1063/1.4891439.1]

surface area of the textured surface to its projected area. A drop of ferrofluid on a flat silicon substrate treated with OTS exhibited ~20° contact angle, which confirms impregnation since θ_c was calculated to be 65° for our sample. As seen in Figure 1(a), a system comprising of a water droplet on this surface would obey the state in which a thin layer of ferrofluid-lubricant cloaks the water droplet.[36,44] The oil-based ferrofluid is immiscible with water, thus allowing for the droplet to rest on the surface with a ferrofluid cloak stably. As confirmed by the photograph in Figure 1(b), when the spreading coefficient of the ferrofluid on water in the presence of vapor is positive, the ferrofluid will spread on the droplet, i.e., $S_{ow(v)} \geq 0$, where $S_{ow(v)} = \gamma_{wv} - \gamma_{ov} - \gamma_{ow}$ and γ_{wv}, γ_{ov}, γ_{ow} are the respective interfacial tensions of the water-air, ferrofluid-air, and ferrofluid-water interfaces.

Since the contact angle of the ferrofluid on the solid in the presence of water was measured to be zero, $\theta_{os(w)} = 0^{\circ}$, or $S_{os(w)} \geq 0$, the ferrofluid will fully spread on the micropost tops beneath a water droplet, thus leading to virtually no droplet pinning. This results in extremely low contact-angle hysteresis (~1°) and high droplet mobility. Approaching a permanent magnet (K&J Magnetics) to the droplet on this surface as shown in Figure 1(c) causes the droplet to accelerate towards the magnet (see supplementary material video for Figure 1(c)).[59] The droplet position versus time was tracked and recorded in Figure 1(d), which shows that the droplet accelerates towards the region of highest magnetic field.

Now, to better understand the mechanism behind droplet propulsion, we imaged single droplets resting on the surface at high magnification. In our experiments, as seen in Figure 2(a), we first approached the magnet symmetrically above the droplet. The droplet is seen to deform towards the magnet, and the magnetic particles crowd to form local cone-like structures. The magnetic attractive force is locally balanced by restoring interfacial forces that act to hold these particles in the cloak. In this symmetric configuration, the droplet remains stationary, as there is no net horizontal force on the droplet. However, when the magnet is in an asymmetric configuration, the droplet is seen to both distort and translate towards the region of higher magnetic field. As sketched in Figure 2(b), the cone-like structures are seen to orient along the direction of the maximum field intensity (along the centerline of the magnet), which explains the droplet distortion in the same direction. We measure the distortion of the droplet, $\theta_{dropletorientation}$ for various magnet orientations, θ_{magnet}, and indeed, the droplet is seen deform at an angle that aligns with the center of the magnet surface. This asymmetric

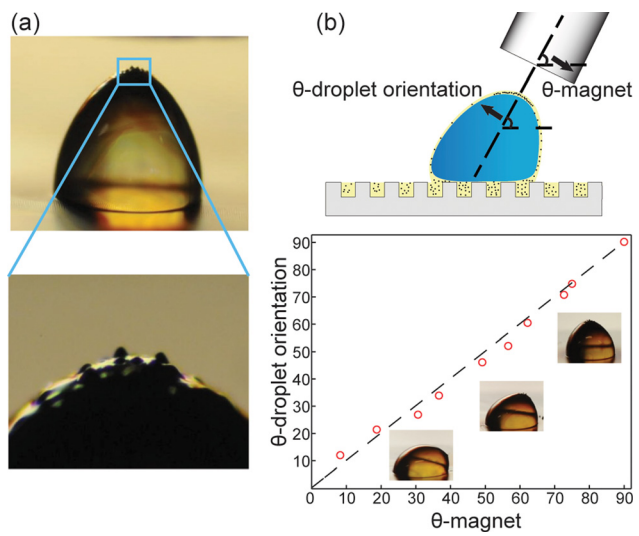

FIG. 2. (a) Symmetric magnet configuration. Magnetic particles cluster over the cloaked water droplet and orient themselves to be directly underneath the region of highest magnetic field intensity. (b) Asymmetric magnet configuration. Magnet approaching angle versus droplet orientation angle which shows that the clumped particles act to deform the droplet directly in the direction of highest field intensity, or directly at the angle the magnet is being approached.

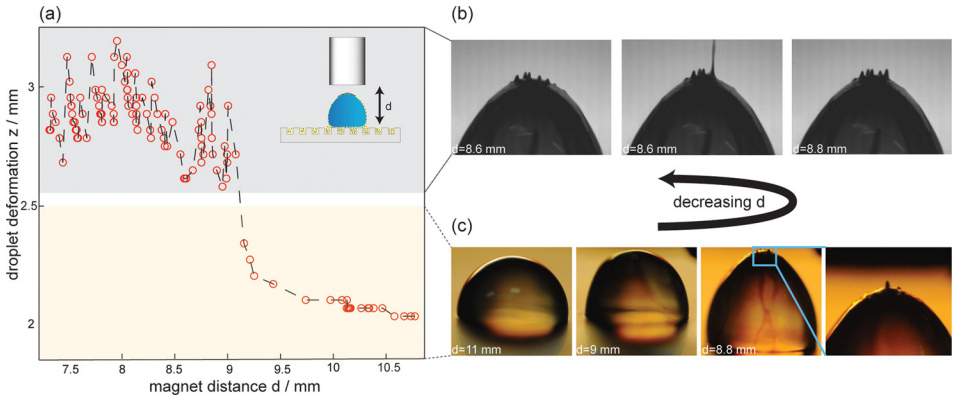

FIG. 3. Jetting transition of ferrofluid-cloaked droplet. (a) Droplet deformation versus magnet distance. Droplet height continuously increases until critical jetting transition distance is reached. Droplet height then begins to fluctuate as fluid jets grow and detach repeatedly from cloak/air interface. (b) High-Speed images of fluid jet detaching from cloak/air interface in the jetting regime.[59] (c) Snapshots of droplet deformation as the magnet is slowly approached to the surface (Multimedia view). [URL: http://dx.doi.org/10.1063/1.4891439.2]

interaction results in a net horizontal force on the droplet, which serves to propel the drops.

Cloaked droplets continue to deform along with the ferrofluid until the magnet reaches a critical distance at which the magnetic attractive force of the particles is greater than the interfacial forces that are stabilizing them in the cloak. The particles then physically detach from the film and agglomerate on the surface of the magnet, thus marking the onset of the "jetting" transition in a manner consistent with the jetting of particles from a free ferrofluid surface reported previously.[58] Applying scaling analysis, one can roughly predict the required condition for which jetting transition occurs.[58] As shown in Ref. 58, the natural scaling for the interfacial deflection of the ferrofluid

$$h_c{}^2 = \frac{\mu_o \chi M^2 R_m{}^6 V}{18\pi\gamma d^6}, \tag{2}$$

where $h_c = O(10^{-3}m)$ is a characteristic interfacial distortion during a jetting experiment, $\mu_0 = 1.257 \times 10^{-6} mkgs^{-2}A^2$ is the permeability of free space, magnetic susceptibility $\chi = 6.79$, permanent magnet magnetization $M = O(10^6 A/m)$, radius of magnet $R_m = 3 \times 10^{-3}m$, characteristic volume of clumped particle area $V = O(10^{-10}m^3)$, interfacial tension $\gamma = 0.022N/m$, and magnet distance from unperturbed interface d.[58] Solving Eq. (2) for d utilizing the given values for the other quantities, we can predict a critical magnet distance of $d = O(10^{-2}m)$ for the jetting transition to occur, which we confirm experimentally. A high-speed camera was used to visualize this phenomenon as shown in Figure 3(b), and in supplementary material.[59] The droplet height was recorded as the distance between the magnet, and the droplet was decreased, and is graphically displayed in Figure 3(a). We observe two different regimes in the droplet deformation as shown in the plot.

When the distance between the magnet and droplet was larger than the critical jetting length, the droplet deforms smoothly and reaches an equilibrium deformation. When the distance is shorter, the particles begin to jet from the cloak, and the droplet height or deformation begins to oscillate due to the continuous forming and detaching of liquid jets. This accounts for the fluctuating data points on the left portion of the graph. This jetting phenomenon restricts the magnitude of the magnetic field that could be used for droplet manipulation and should be taken into consideration while designing these systems.

To highlight the potential technological impact of this type of active surface, we present experiments including free

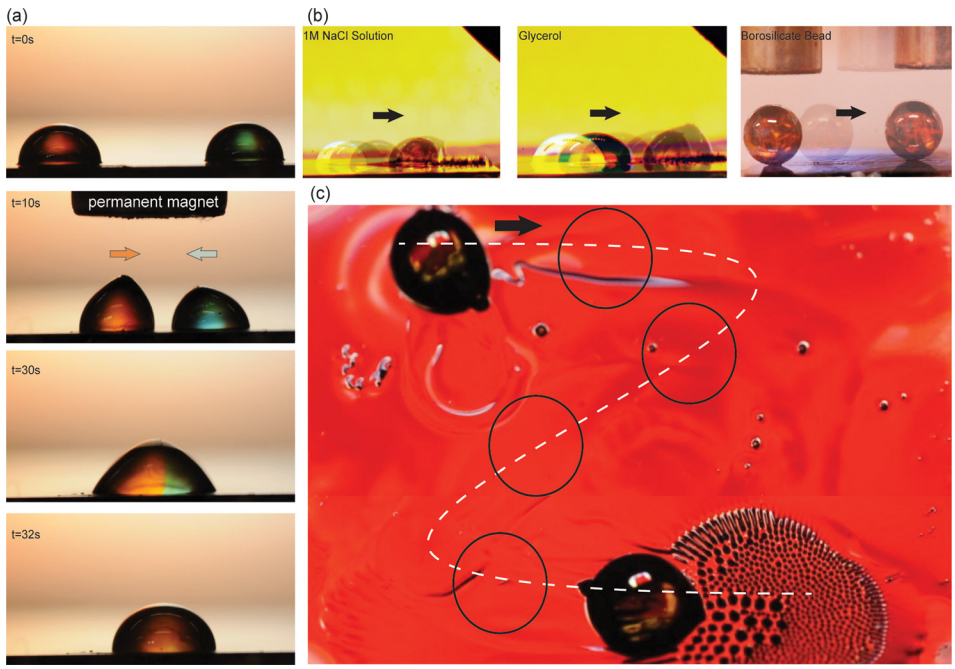

FIG. 4. (a) Two water droplets (dye used to color droplets) are placed on ferrofluid-infused surface. A magnet is lowered vertically directly between droplets and causes them to move toward one another. Coalescence of droplets occurs and is captured just before droplets fully mix. (b) Droplets of various fluids and one solid are actuated and displaced when a permanent magnet is approached to the surface. (c) Water droplet being dragged along an s-curve as the magnet is held beneath the surface.

droplet coalescence, movement of viscous and conductive fluids as well as solid particles, and moving objects on complex curved paths. Simply introducing a magnet centered between two droplets may induce coalescence (Figure 4(a)). The region of highest magnetic field intensity, directly beneath the magnet, attracts both droplets to center under the magnet, leading to coalescence. Additionally, the motion of conductive liquids (1 M NaCl aqueous solution) and highly viscous dielectric liquids (100% glycerol) was achieved and displayed in Figure 4(b). The manipulation of low surface tension fluids could be achieved with this method utilizing the appropriate immiscible lubricant, which can be a challenge with typical superhydrophobic surfaces unless they have complex textures.[4] The proposed surfaces along with magnets can also be used for manipulating solid objects on surfaces. As demonstrated in Figure 4(b), a 5 mm glass bead is translated on the surface using a permanent magnet. Finally, for lab-on-a-chip applications, pre-fabricated microfluidic channels or embedded electrodes[23] would be used to move and mix droplets along complex paths, yet this surface's droplet actuation mechanism naturally does not have constraints on path geometries (Figure 4(c)). Therefore, ferrofluid-impregnated surfaces provide a framework for free surface manipulation of a broad range of liquids with various physicochemical, electrical, and magnetic properties.

We thank the MIT-KFUPM Center for Clean Water and Clean Energy for financial support.

[1]P.-G. de Gennes, *Capillarity and Wetting Phenomena: Drops, Bubbles, Pearls, Waves* (Springer, New York, 2004).
[2]D. Quéré, Annu. Rev. Mater. Res. **38**, 71 (2008).
[3]X. Deng, L. Mammen, H.-J. Butt, and D. Vollmer, Science **335**, 67 (2012).
[4]A. Tuteja, W. Choi, M. Ma, J. M. Mabry, S. A. Mazzella, G. C. Rutledge, G. H. McKinley, and R. E. Cohen, Science **318**, 1618 (2007).
[5]J. C. Bird, R. Dhiman, H.-M. Kwon, and K. K. Varanasi, Nature **503**, 385 (2013).
[6]C. Duez, C. Ybert, C. Clanet, and L. Bocquet, Nat. Phys. **3**, 180 (2007).
[7]A. J. Meuler, G. H. McKinley, and R. E. Cohen, ACS Nano **4**, 7048 (2010).
[8]S. Jung, M. K. Tiwari, N. V. Doan, and D. Poulikakos, Nat. Commun. **3**, 615 (2012).
[9]J. Lv, Y. Song, L. Jiang, and J. Wang, ACS Nano **8**, 3152 (2014).
[10]T. Maitra, M. K. Tiwari, C. Antonini, P. Schoch, S. Jung, P. Eberle, and D. Poulikakos, Nano Lett. **14**, 172 (2014).
[11]P. Guo, Y. Zheng, M. Wen, C. Song, Y. Lin, and L. Jiang, Adv. Mater. **24**, 2642 (2012).
[12]J. B. Boreyko and C. P. Collier, ACS Nano **7**, 1618 (2013).
[13]J. Boreyko and C. Chen, Phys. Rev. Lett. **103**, 184501 (2009).
[14]N. A. Patankar, Soft Matter **6**, 1613 (2010).
[15]C. Dorrer and J. Rühe, Adv. Mater. **20**, 159 (2008).
[16]D. M. Anderson, M. K. Gupta, A. A. Voevodin, C. N. Hunter, S. A. Putnam, V. V. Tsukruk, and A. G. Fedorov, ACS Nano **6**, 3262 (2012).
[17]N. Miljkovic, R. Enright, Y. Nam, K. Lopez, N. Dou, J. Sack, and E. N. Wang, Nano Lett. **13**, 179 (2013).
[18]Y. Koc, A. J. de Mello, G. McHale, M. I. Newton, P. Roach, and N. J. Shirtcliffe, Lab Chip **8**, 582 (2008).
[19]W. Choi, M. Hashimoto, A. K. Ellerbee, X. Chen, K. J. M. Bishop, P. Garstecki, H. A. Stone, and G. M. Whitesides, Lab Chip **11**, 3970 (2011).
[20]P. Tabeling, Curr. Opin. Biotechnol. **25**, 129 (2014).
[21]O. D. Velev, B. G. Prevo, and K. H. Bhatt, Nature **426**, 515 (2003).
[22]D. R. Link, E. Grasland-Mongrain, A. Duri, F. Sarrazin, Z. Cheng, G. Cristobal, M. Marquez, and D. A. Weitz, Angew. Chem. Int. Ed. **45**, 2556 (2006).
[23]D. 't Mannetje, S. Ghosh, R. Lagraauw, S. Otten, A. Pit, C. Berendsen, J. Zeegers, D. van den Ende, and F. Mugele, Nat. Commun. **5**, 3559 (2014).
[24]H. Mertaniemi, V. Jokinen, L. Sainiemi, S. Franssila, A. Marmur, O. Ikkala, and R. H. A. Ras, Adv. Mater. **23**, 2911 (2011).
[25]S. Daniel, M. K. Chaudhury, and P.-G. de Gennes, Langmuir **21**, 4240 (2005).
[26]P. Brunet, J. Eggers, and R. Deegan, Phys. Rev. Lett. **99**, 144501 (2007).
[27]C.-C. Huang, M. Z. Bazant, and T. Thorsen, Lab Chip **10**, 80 (2010).
[28]M. Z. Bazant, M. S. Kilic, B. D. Storey, and A. Ajdari, Adv. Colloid Interface Sci. **152**, 48 (2009).
[29]S.-K. Fan, T.-H. Hsieh, and D.-Y. Lin, Lab Chip **9**, 1236 (2009).
[30]K. Piroird, C. Clanet, and D. Quéré, Phys. Rev. E **85**, 056311 (2012).
[31]J. V. I. Timonen, M. Latikka, L. Leibler, R. H. A. Ras, and O. Ikkala, Science **341**, 253 (2013).
[32]J. Yan, K. Chaudhary, S. C. Bae, J. A. Lewis, and S. Granick, Nat. Commun. **4**, 1516 (2013).
[33]I. F. Lyuksyutov, D. G. Naugle, and K. D. D. Rathnayaka, Appl. Phys. Lett. **85**, 1817 (2004).
[34]E. Beaugnon and R. Tournier, Nature **349**, 470 (1991).
[35]Y. Ikezoe, N. Hirota, J. Nakagawa, and K. Kitazawa, Nature **393**, 749 (1998).
[36]J. D. Smith, R. Dhiman, S. Anand, E. Reza-Garduno, R. E. Cohen, G. H. McKinley, and K. K. Varanasi, Soft Matter **9**, 1772 (2013).
[37]D. Quéré, Rep. Prog. Phys. **68**, 2495 (2005).
[38]A. Lafuma and D. Quéré, EPL **96**, 56001 (2011).
[39]T.-S. Wong, S. H. Kang, S. K. Y. Tang, E. J. Smythe, B. D. Hatton, A. Grinthal, and J. Aizenberg, Nature **477**, 443 (2011).
[40]A. Eifert, D. Paulssen, S. N. Varanakkottu, T. Baier, and S. Hardt, Adv. Mater. Interfaces **1**, 1300138 (2014).
[41]A. Carlson, P. Kim, G. Amberg, and H. A. Stone, EPL **104**, 34008 (2013).
[42]X. Huang, J. D. Chrisman, and N. S. Zacharia, ACS Macro Lett. **2**, 826 (2013).
[43]H. Liu, P. Zhang, M. Liu, S. Wang, and L. Jiang, Adv. Mater. **25**, 4477 (2013).
[44]S. Anand, A. T. Paxson, R. Dhiman, J. D. Smith, and K. K. Varanasi, ACS Nano **6**, 10122 (2012).
[45]K. Rykaczewski, A. T. Paxson, M. Staymates, M. L. Walker, X. Sun, S. Anand, S. Srinivasan, G. H. McKinley, J. Chinn, J. H. J. Scott, and K. K. Varanasi, Sci. Rep. **4**, 4158 (2014).
[46]R. Xiao, N. Miljkovic, R. Enright, and E. N. Wang, Sci. Rep. **3**, 1988 (2013).
[47]S. B. Subramanyam, K. Rykaczewski, and K. K. Varanasi, Langmuir **29**, 13414 (2013).
[48]P. Kim, T.-S. Wong, J. Alvarenga, M. J. Kreder, W. E. Adorno-Martinez, and J. Aizenberg, ACS Nano **6**, 6569 (2012).
[49]L. Chen, A. Geissler, E. Bonaccurso, and K. Zhang, ACS Appl. Mater. Interfaces **6**, 6969 (2014).
[50]A. K. Epstein, T.-S. Wong, R. A. Belisle, E. M. Boggs, and J. Aizenberg, Proc. Natl. Acad. Sci U.S.A. **109**, 13182 (2012).
[51]S. B. Subramanyam, G. Azimi, and K. K. Varanasi, Adv. Mater. Interfaces **1**, 1300068 (2014).
[52]J. Li, T. Kleintschek, A. Rieder, Y. Cheng, T. Baumbach, U. Obst, T. Schwartz, and P. A. Levkin, ACS Appl. Mater. Interfaces **5**, 6704 (2013).
[53]E. Ueda and P. A. Levkin, Adv. Healthcare Mater. **2**, 1425 (2013).
[54]L. Xiao, J. Li, S. Mieszkin, A. Di Fino, A. S. Clare, M. E. Callow, J. A. Callow, M. Grunze, A. Rosenhahn, and P. A. Levkin, ACS Appl. Mater. Interfaces **5**, 10074 (2013).
[55]R. E. Rosensweig, Sci. Am. **247**, 136 (1982).
[56]R. E. Rosensweig, Annu. Rev. Fluid Mech. **19**, 437 (1987).
[57]T. A. Franklin, "Ferrofluid Flow Phenomena," MS thesis (Massachusetts Institute of Technology, 2003).
[58]S. S. H. Tsai, I. M. Griffiths, Z. Li, P. Kim, and H. A. Stone, Soft Matter **9**, 8600 (2013).
[59]See supplementary material at http://dx.doi.org/10.1063/1.4891439 for Figure 1(c), which displays a typical droplet mobility experiment, where the droplet is accelerated towards the magnet, and for Figure 3(b), which displays a high-speed video of a ferrofluid jet detaching from the ferrofluid cloak.